

## HIGH TEMPERATURE SURFACE PARAMETERS FOR SOLAR POWER

C. P. Butler, R. J. Jenkins, R. L. Rudkin and F. I. Laughridge  
U. S. Naval Radiological Defense Laboratory, San Francisco 24, California

### ABSTRACT

A method has been developed for measuring the solar absorptance and total hemispherical emittance of surfaces up to 800°C using an arc image furnace. These parameters have been measured over the temperature range of 200°C to 800°C for six polished and eight coated metals. The thermal conversion efficiency of a surface as a receiver for solar radiant energy in a power generator depends primarily on the absorptance and the ratio of the emittance and concentration ratio at a given distance from the sun. Thermal conversion efficiencies with a concentration ratio of 50 have been computed for each surface when exposed to solar radiation at the Earth's mean orbital radius. The most promising coatings of those investigated, which were applied with a plasma jet, are crystalline tungsten and granular molybdenum whose efficiencies range from approximately 95% at 200°C to 30% at 800°C.

### INTRODUCTION

Direct photovoltaic conversion of sunlight to electrical energy has been successfully used in some satellites as a primary source of power. Another possible source of power is some form of heat engine or thermoelectric generator utilizing solar energy. The efficiency of such a device can be maximized by the proper selection of coating materials for the receiving surface.

One fundamental problem in using the radiant energy of the sun to drive a heat engine is the control of the spectral properties of the receiving or absorbing surface exposed to the sun's rays. Such a surface must have a high absorptance at those wave lengths at which the sun radiates, but a low emittance for those wave lengths at which re-emission occurs.

This study is confined to the behavior of real surfaces under simulated solar radiation conditions of space. A judicious selection of materials for a coating as well as the substrate to support it should produce a selective surface which will operate at high temperatures. The purpose of

# Contrails

this work is to find a combination of materials which will yield a high thermal conversion efficiency over the temperature range 200°C to 800°C.

## EQUILIBRIUM TEMPERATURES OF SURFACES IN SPACE

The equilibrium temperature of any object orbiting in space is partly a function of the ratio of the absorptance of solar radiation falling on one side and the emittance of the object from all sides. At pressures corresponding to a hundred miles or more above the surface of the earth, gaseous conduction is so low that convective cooling of a hot surface is negligible. Under steady state conditions, such as a meteor or a dead satellite, where no heat is generated nor used internally, heat conduction likewise will be zero. The only mechanism for heat transfer is by absorption of solar energy and reradiation of this same energy.

The radiant energy,  $H$ , in  $\text{cal cm}^{-2} \text{sec}^{-1}$  outside the earth's atmosphere is called the solar constant and varies inversely with the distance from the sun. A surface of projected area  $S_1$  (in  $\text{cm}^2$ ) when exposed normally to the sun's rays will absorb energy at a rate,  $Q_1$ , depending on its absorptance,  $\alpha$ , thus

$$Q_1 = \alpha S_1 H \quad (1)$$

The exposed surface will rise in temperature because of the absorption of solar energy and will radiate at a rate,  $Q_2$ , depending on its hemispherical emittance,  $\epsilon$ , and its absolute temperature,  $T$ , thus

$$Q_2 = \epsilon S_2 \sigma (T^4 - T_0^4) \quad (2)$$

where  $\sigma$  is the Stefan-Boltzman constant,  $S_2$  is the radiating area, and  $T_0$  is the temperature of space or the temperature of the surface facing the receiver. For all calculations here,  $T_0$  will be assumed zero, and no part of the field of view of the receiving surface will include the surface of a planet.

At equilibrium,  $Q_1$  will equal  $Q_2$ , and the equilibrium temperature of the receiving surface from Equations (1) and (2) is

$$T = \left[ \frac{S_1 \alpha H}{S_2 \epsilon \sigma} \right]^{1/4} \quad (3)$$

In this case, when a thin flat plate is positioned normally to the sun's rays, the area radiating is twice the area exposed to solar radiation, and Equation (3) becomes

$$T = \left[ \frac{\alpha H}{2 \epsilon \sigma} \right]^{1/4} \quad (4)$$

# Contrails

Figure 1 is a plot of Equation (4) to demonstrate the effect of varying the ratio  $\alpha/\epsilon$  for a flat plate at four different orbital distances from the sun corresponding to Mercury, Venus, Earth and Mars. Table I gives the planetary data from which the irradiances at various distances can be calculated.

If a collecting mirror or lens is used to focus the rays of the sun on the receiving surface, the irradiance will be increased. It is convenient to define a multiplying or concentrating factor,  $m$ , or the product of the radiant energy concentration of the optical system and the ratio of the projected receiving area and the reradiating area. In this case a thin plate with no optical concentration would have an  $m$  value of  $1/2$  while a sphere under the same conditions would have an  $m$  value of  $1/4$ .

Equilibrium temperatures for various geometries and collecting systems are shown in Fig. 2 which is computed for a receiving surface exposed at the earth's mean distance from the sun. In these calculations it should be noted that the absolute values of  $\alpha$  and  $\epsilon$  do not enter into the equations. The temperatures are correct whether the absorptance is 1.0 or 0.1. However, if any of the heat generated in the receiver is used, no matter how small, the above calculations no longer apply.

## EFFICIENCIES AND TEMPERATURES

Any type of solar power generator will probably employ a flat receiving surface at the focus of a mirror or a lens. As this surface is heated, the temperature gradient between it and a heat sink behind it can be used as the source of power in a heat engine. Since the efficiency of any heat engine is determined by the Carnot cycle, high temperatures mean better efficiencies. An arbitrary goal of  $800^{\circ}\text{C}$  was chosen for this work, a temperature for which there are available a number of stable materials.

The maximum working temperature of an irradiated surface depends not only on its optical properties, but also on how much power is extracted, i.e., rate of heat flow,  $W$ , from the surface into the engine. This power is in addition to that lost by radiation from the surface, so that Equation (1) for an equilibrium temperature now becomes

$$Q_1 = Q_2 + W \quad (5)$$

or including the concentration factor  $m$ ,

$$m\alpha SH = \epsilon S\sigma T^4 + W \quad (6)$$

For any system employing a single surface, the absorbing and emitting areas are identical.

# Contrails

The efficiency,  $\beta$ , of a solar absorbing surface for a power generator has been defined as<sup>1</sup> the ratio of the rate of heat conducted from the surface and the total amount of incident radiant power in the solar beam, thus

$$\beta = \frac{W}{mHS_1} \quad (7)$$

In practice, of course, there would be conductive losses to the structure holding the receiver, radiative losses from the sides, etc., so that the ideal situation is represented here, where the only losses are those by radiation of the surface itself.

Combining Equations (6) and (7), we have

$$\beta = \alpha - \frac{\epsilon}{m} \left( \frac{\sigma T^4}{H} \right) \quad (8)$$

This equation is of fundamental importance in the design of any solar power generator and shows immediately that the efficiency can never exceed the absorptance, regardless of the emittance. Furthermore, the ratio of the emittance and the concentration or collecting factor,  $m$ , will determine the efficiency at a given absorptance. These relationships can be readily seen in Fig. 3 which shows how the temperature depends on  $\alpha$  and on  $\epsilon/m$ . When the efficiency of a solar generator is zero, we have the equilibrium condition which can be verified by comparing with Figs. 1 and 2, in which only the ratio  $\alpha/\epsilon$  determines the temperature. The rapid drop in efficiency at the higher temperatures reflects the fact that the radiation loss from the receiver increases as the fourth power of the temperature.

## ABSORPTANCE AND EMITTANCE

At any likely distance from the sun at which a satellite would operate, the solar rays may be considered collimated, as shown in Table I under the heading  $f$ /ratio. Even for Mercury, the  $f$ /ratio of the sun as seen from that distance is still only 42, corresponding to a subtended angle of approximately 1-1/2 degree, or about three times the angular diameter of the sun as seen from the earth.

If a collecting mirror or lens is used, the angle of convergence on the receiver will be greater than these figures by an amount depending on the concentration desired. The  $f$ /ratio shown in the table for the NRDL source is that which corresponds to the distance of the sun at an irradiance of  $6.3 \text{ cal cm}^{-2}\text{sec}^{-1}$ . The convergence of the laboratory source used to simulate the sun is greater, which represents more nearly an optical system which might be used in real solar generators.

Absolute values of emittance on the other hand must hold over  $2\pi$  steradians. An absorbing surface for solar power generation on a

# Contrails

satellite, whether it faces outward or inward at the focus of a collecting mirror, is free to radiate energy in all directions. It is essential, therefore, that all calculations such as those given above refer to the hemispherical emittance and not the normal emittance.

## SPECTRAL SELECTIVITY

The radiating temperature of the sun, as deduced from both spectral and total radiation measurements of the solar photosphere, is close to 6000°K for which the maximum emission falls at a wave length of approximately 0.5 microns.<sup>2</sup> Its spectral distribution does not change with distance, but will be altered slightly if a collecting mirror or lens system is used to concentrate the solar beam. While not strictly Planckian, for the purpose of studies such as these, the sun will be considered to emit as a black body.

The thermal radiation emitted by a receiver operating at say 500°C takes place at another region of the spectrum. Assuming a grey surface, it will radiate most copiously at 4.0 microns, some 8 times the wave length of the incoming solar radiation. This large difference in wave length between absorption and emission can be utilized in producing a spectrally selective surface. At this temperature, the spectra do not overlap to any great extent, but if the temperature continues to rise, the spectral distribution of the reradiation moves to shorter wave lengths, where more and more of each will coincide. The wave length of maximum emission for the work reported here varies from 2.7 microns at 800°C to 6 microns at 200°C.

## EXPERIMENTAL TECHNIQUES

The radiant energy of the sun is simulated in the laboratory with an arc image furnace. The radiation is emitted from the plasma formed in the positive crater of a 9 mm diameter cored carbon operating at 40 volts and 70 amperes. It has been shown<sup>3</sup> that the radiating temperature of the high intensity carbon arc is approximately 5800°K, which is close to that of the solar photosphere.

Radiant energy from the positive crater is collected by an elliptical mirror, and concentrated onto a thin specimen of the metal under study suspended with fine wires inside an evacuated chamber. The chamber is fitted with a quartz window to admit the arc radiation, and its walls are painted black on the inside to provide surfaces which have an absorptance of nearly unity. Fig. 4 shows a photograph of the vacuum chamber with parts cut away to show the position of the beam and specimen. Chromel-alumel thermocouple wires, 0.005 inches in diameter support the specimen in the focal plane.

# Contrails

Pressures of approximately  $10^{-5}$  mm Hg can be maintained in the chamber during both the heating and cooling cycle by means of a liquid nitrogen cold trap and ion pump. At these pressures, convective losses from the specimen are negligible.<sup>4</sup>

The solar absorptance of the surface of the specimen is given by

$$\alpha = \frac{mc(\dot{T}_1 - \dot{T}_2)}{S_1 H} \quad (9)$$

where  $m$  is the mass of the specimen in grams,  $c$  its specific heat in  $\text{cal g}^{-1} \text{ } ^\circ\text{C}^{-1}$ ,  $\dot{T}_1$  the change in temperature with time during the heating or exposure period,  $\dot{T}_2$  the change in temperature with time during the cooling period,  $S_1$  the projected area of the specimen in  $\text{cm}^2$ , and  $H$  the irradiance of the beam in  $\text{cal cm}^{-2} \text{ sec}^{-1}$ .

The beam irradiance  $H$  is measured by exposing a blackened silver or copper button of the same dimensions in the same chamber and substituting 1.0 for the absorptance in Equation (9).

The total hemispherical emittance of a surface is given by

$$\epsilon = \frac{mc\dot{T}_2}{S_2 \sigma (T^4 - T_0^4)} \quad (10)$$

where  $S_2$  is now the area of the entire specimen,  $\sigma$  the Stefan-Boltzmann constant,  $T$  the temperature of the specimen and  $T_0$  the wall temperature. Since the specimen is small compared to the dimensions of the enclosure, the chamber is effectively an isothermal black body with a Planckian distribution of wall radiation. A minor error is introduced because of the solid angle subtended by the quartz window which cannot be cooled as effectively as the metal walls of the chamber, and in consequence, no measurements are taken below a specimen temperature of  $200^\circ\text{C}$ .

A tracing of an original time-temperature record is shown in Fig. 5, from which both  $\alpha$  and  $\epsilon$  can be calculated.

The temperature to which a specimen can be heated in an image furnace depends on the irradiance of the beam, the absorptance and the heat losses from the specimen. At an irradiance of approximately  $6 \text{ cal cm}^{-2} \text{ sec}^{-1}$  all the specimens tested could be heated to the desired temperature in less than one minute of continuous exposure. For example, the temperature rise in a 2.7 gram specimen of polished gold was  $19^\circ\text{C sec}^{-1}$  at  $800^\circ\text{C}$ .

Typical specimen dimensions are  $3/4$  inch in diameter and 0.040 inches thick. Three 0.013 inch diameter holes are drilled  $120^\circ$  apart around the edge of the specimen. Bare 5 mil thermocouple wires, alumel and chromel are fastened into two of these holes and a third supporting wire in the third. The thermocouple circuit is through the specimen itself, and hence



# Contrails

the output indicates the temperature within the button. All voltages read on the recording potentiometer are referred to  $0^{\circ}\text{C}$  with the cold junction immersed in a Dewar of melting ice.

## MATERIAL REQUIREMENTS

If the receiving surface of a solar generator is designed to operate at a temperature of  $800^{\circ}\text{C}$  in outer space, there are certain basic requirements for the materials. The melting point of the material as well as the coating must lie well above this temperature. The vapor pressure of the material must be low enough at these temperatures so that evaporation will not alter the optical characteristics through thermal etching. And finally, any applied coating must retain its bond with the substrate over the entire temperature range.

## POLISHED SURFACES

Because of the scarcity of data on the hemispherical emittance and solar absorptance of polished metals in this temperature range, measurements of these parameters were made on six common metals. This information is essential before any attempt is made to evaluate the effect of spectrally selective coatings. Even if two specimens have the same composition, there is the further problem of grinding and polishing to a specific emittance. In general, the higher the polish the lower the emittance, but this is a matter of degree, depending on the lap, its speed, the polishing compound, the hardness of the metal, etc. This may be one reason why values of the emittance as found in the literature are not always consistent. A second reason is that many freshly polished metal surfaces oxidize rapidly in air.

Each specimen was cut to size, drilled, ground with 600 grit Carborundum, and polished on a wet cloth lap with either Linde Alumina Type B-5125 or unlevigated jewelers rouge. The polishing was carried to the point where a good specular reflection could be seen. Each specimen was then mounted as soon as possible in the vacuum chamber and pumping begun.

The metals selected, all of whose melting points lie well above  $800^{\circ}\text{C}$ , are as follows:

1. Silver; commercial rolled plate (999 + fine)
2. Gold; commercial grade (99.95 percent fine)
3. Nickel; commercially pure, rod
4. Armco Iron; (C 0.014, Mn 0.032, P 0.003, S 0.017, Si 0.003, Cu 0.11 percent)
5. Molybdenum; vacuum arc cast, machined, extruded, recrystallized, rolled.
6. Tantalum; commercially pure, arc cast or sintered, rod.

# Contrails

## RESULTS

Evaluation of the performance of the chamber, of the specimen mounting and of the input energy of the carbon arc was accomplished by mounting platinum blackened specimens of copper and silver in the chamber and comparing the measured specific heats with those found in the literature. It was concluded that in the temperature range of 200°C to 800°C, the confidence limit is approximately 10% or better.

All results on absorptance and emittance measurements of polished metals are shown in Figs. 6 through 11. The efficiency of these same surfaces as receivers for a solar generator is shown in Fig. 12, calculated for the solar constant at the earth's mean distance and a magnification of 50.

Two sets of data are shown for the emittance of polished silver. This is an example of the effects of thermal etching which is pronounced in a material like silver. Its vapor pressure<sup>5</sup> at the high temperature is nearly equal to that of its environment so that evaporation proceeds rapidly. This process increases the emittance as shown by the upper curve in Fig. 6. Copper likewise undergoes thermal etching at elevated temperatures.<sup>4</sup>

The normal emittance of nickel, tantalum and molybdenum<sup>6</sup> as a function of temperature is generally lower than the results reported here, but there is no apparent consistency between them. This simply emphasizes the statement that at present hemispherical emittances cannot be calculated from the normal.

## COATED SURFACES

When the analytical and experimental basis for measuring and evaluating the high temperature properties of polished surfaces was completed, a search for suitable coatings was begun. These coatings must meet the same requirements given above, besides improving the thermal efficiency of the surface.

Even though silver as a substrate for a coating was recognized as inherently unstable, a  $\text{Ag}_2\text{S}$  coating was deposited on a polished specimen of silver. This was chosen because  $\text{Ag}_2\text{S}$  is black, i.e., has an absorptance near 1.0, is readily prepared, and was one of the first surface coatings proposed by Tabor.<sup>7</sup>

The coating was applied electrolytically at a potential of 9 volts for 45 seconds from a solution of

Thioacetamide	10 gr
Saturated $\text{Na}_2\text{CO}_3$	5 ml
Distilled water to make	100 ml



# Contrails

After the coating was dried and buffed, it appeared quite black with a bright specular reflectance.

The data presented in Fig. 13 refers to the second cycle only for this coating. The coating gradually evaporated, leaving the original brightly polished silver surface which has a low absorptance. At 800°C its life is less than 5 minutes, but its stability at lower temperatures was not measured.

Polished molybdenum has an emittance near 0.10, and since its melting point is high, no thermal etching would be expected, nor was any observed at 800°C. The reflection coefficients of carbon black reported in Reference 8, if applied to a stable substrate with a low emittance, looked promising. Carbon blacks are partially transparent in the infrared, and since carbon has a very high melting point, it should make a stable coating.

A very thin coating of carbon black was deposited on a polished molybdenum specimen from the flame of burning kerosene. The resulting coating was dark and appeared like a black specular mirror with a brownish hue. The results for carbon blackened molybdenum are shown in Fig. 14. The coating is apparently stable and shows no tendency to flake, although it is very fragile and cannot be touched.

Armco ingot iron, with a melting point of 1539°C and a low vapor pressure at 800°C, should be an ideal substrate material. Except for the phase change,  $A_2$ , at the Curie point at 768°C, there are no other transformation temperatures below 800°C.<sup>9</sup> It is also easy to work, is readily available, and there is a large volume of published data on its characteristics.

The mechanical method of producing a spectrally selective coating visualized a controlled etching of the polished surface. If pits can be formed in the surface whose dimensions are small compared to the wave length at which emittance occurs, a selective surface should be produced.

A polished specimen was etched by sandblasting with a jet of SS White Abrasive No. 2 until the surface exhibited a matte finish. The results are shown in Fig. 15.

The "bluing" of steel is an old technique in which a controlled oxide layer is formed on a polished iron or steel surface by immersing in a niter bath for a specified time. A specimen of polished Armco iron was blued by this method and its optical characteristics measured, as shown in Fig. 16. The data presented here is for the first two cycles only since the oxide layer evaporated at the high temperature, lowering the absorptance toward the value for the polished metal. It is interesting to note that the emittance of this coated specimen was very nearly that of the original polished surface, indicating that the coating was very nearly transparent to all wave lengths greater than about 2 microns. The conversion efficiency for these four coatings is shown in Fig. 17.

Plasma flame spraying equipment now available commercially is designed to apply high temperature materials to a metal substrate. The powdered

# Contrails

metal is fed through the high current arc in a stream of nitrogen and hydrogen and is projected onto the work either in the vapor form or as fine molten droplets. Coatings of many refractory metals can be built up on a base metal such as iron or steel where a high temperature resistant coating is required.

This method of applying a stable coating to surfaces suggests that an optically selective layer could be sprayed onto a specular metal surface which would behave much as a controlled etching.

Armco iron specimens which were cut to size and fine ground were plasma flame sprayed with four different compounds in a preliminary attempt to evaluate the optical characteristics of such a coating. Usually the base metal is sandblasted prior to spraying, but in this instance, the refractory materials were applied directly to the fine ground surface of the specimens. These coatings showed no tendency to crack or peel at the elevated temperatures and are considered satisfactory for a receiving surface.

It should be emphasized that the application of refractory coatings with a plasma flame is an art. The arc voltage and current, the gas carrier pressure, the mesh size of the powder, the distance between the jet orifice and the work, the temperature of the metal being sprayed, and the time are all factors affecting the type of coating. The coatings reported here were made with two passes, one horizontally and the other vertically across the specimen to give an even coating. The uniformity was judged by eye only.

Four coatings on Armco iron were produced as follows:

1. Granular molybdenum, -140 mesh  $\pm$  325 mesh, Metco XP-1103
2. Tungsten carbide, 12% cobalt aggregate, -270 mesh +15 micron, Metco XP-1110.
3. Crystalline tungsten, -200 mesh +30 micron, Metco XP-1106.
4. 60% Chromium carbide-cobalt blend, Metco XP-1109

The results for these coatings is shown in Figs. 18, 19, 20 and 21. Their efficiencies are shown in Fig. 22.

All efficiencies calculated for the surfaces reported have been done with a **concentration** ratio of 50. This was arbitrarily chosen to display the differences between the surfaces. At other values of  $m$ , these differences have a slightly different appearance, i.e., some surfaces will appear in a different relative position. However, at this figure the curves represent what can be expected at a temperature of 800°C.

The 60% chromium carbide - cobalt blend was unstable at the high temperature and the results shown are for the first two cycles only. Further cycling lowered the absorptance and a subsequent visual inspection indicated that some change had taken place in the coating.

# Contrails

The other three refractory coatings showed no indication of flaking, nor change in optical properties during the runs.

## EFFICIENCIES AT HIGH TEMPERATURES

From the preceding results it can be seen that it is possible to attain thermal conversion efficiencies as high as 40% at 800°C with an irradiance 50 times that of the solar constant at the earth's mean distance from the sun. If a similar calculation is carried out for  $m$  values less than 50, correspondingly lower efficiencies will be found. For example, the efficiency of the granular molybdenum coating given above in direct sunlight with no optics is 35% at 200°C and drops to 0% at 250°C. In this case, either the receiver must be located closer to the sun than the orbit of Mercury, or optical means must be provided to increase the solar irradiance to reach a temperature of 800°C. There is no reason to choose the factor 50 other than convenience in comparing the various coatings on the same scale.

Figure 3 shows that with no optics, a surface would require an absorptance of 1.00 and an emittance of 0.01 at 800°C to reach the same efficiency as found for the coatings given above. While it may be possible to produce such a surface, increasing the solar irradiance will accomplish the same result with the coatings reported here.

## CONCLUSIONS

A surface designed to operate as a receiver for a solar generator up to a temperature of 800°C must be made of materials which have melting points well above this temperature, vapor pressures which are low, and absorptances which are high.

The thermal conversion efficiency of an absorbing surface depends primarily on the absorptance and the ratio of the emittance and concentration. It has been shown that to reach a temperature of 800°C with the coatings reported here, it is essential that the solar irradiance at the earth's distance be increased by optical means.

The solar absorptance and hemispherical emittance of polished silver, gold, nickel, Armco iron, molybdenum and tantalum yield thermal conversion efficiencies of 6% to 23% at 800°C with a concentration ratio of 50. Four coatings, carbon particles on polished molybdenum, Ag<sub>2</sub>S on silver, sand-blasted Armco iron, and blued Armco iron yield efficiencies from 20% to 26% under the same conditions.

Three plasma flame sprayed coatings of granular molybdenum, tungsten carbide and crystalline tungsten on Armco iron yield efficiencies from 25% to 38% at 800°C under the same conditions. At 200°C the efficiencies

# Contrails

of the first two are approximately 95%.

For high temperature applications, the plasma flame sprayed refractory coatings are the most stable and yield the highest efficiencies.

## REFERENCES

1. Jenkins, R. J. "Solar Radiation Receiving Surfaces for Satellite Electrical Power Generators" U. S. Naval Radiological Defense Laboratory Technical Report, USNRDL-TR-434, May 1960.
2. Johnson, F. S., J. of Met., Vol. II, No. 6, Dec. 1954.
3. Davis, T. P. "High Temperature - A Tool for the Future", p. 14, Stanford Research Institute, 1956.
4. Butler, C. P. and Inn, E. C. Y. Surface Effects on Spacecraft Materials, John Wiley and Sons, 1960.
5. Dushman, S. Scientific Foundation of Vacuum Technique, John Wiley and Sons, 1949.
6. Goldsmith, A. and Watermann, T. E. "Thermophysical Properties of Solid Materials", WADC-TR 58-476, 1958.
7. Tabor, H. Bul. Israel Council of Research, Sec. A, Vol. 5A, No. 5, 1956.
8. Kozyrev, B. P. and Vershinin, O. E. Optics and Spectroscopy, Vol. VI, No. 4, April 1959.
9. Kenyon, R. L. Metals Handbook, p. 423, ASME, 1948.

# Contrails

TABLE I

Solar Radiation Data

Planet	Mean orbital radius, $10^6$ miles	$\left[ \frac{R_0}{R} \right]^2$ **	H (cal $\text{cm}^{-2}\text{sec}^{-1}$ )	f/ratio*** of sun
NRDL Arc*	6.7	190.	6.30	8
Mercury	36.0	6.66	0.220	42
Venus	67.2	1.91	0.063	78
Earth	92.9	1.00	0.033	107
Mars	141.5	0.43	0.014	164

\* The data in this row corresponds to an orbital distance simulated by the irradiance of the carbon arc source.

\*\* This corresponds to the (m) in equation (6) where  $R_0$  is the distance of the earth and R that of planet from the sun.

\*\*\* This is the same concept as used in photography, i.e., the distance of the planet from the sun divided by the solar diameter.

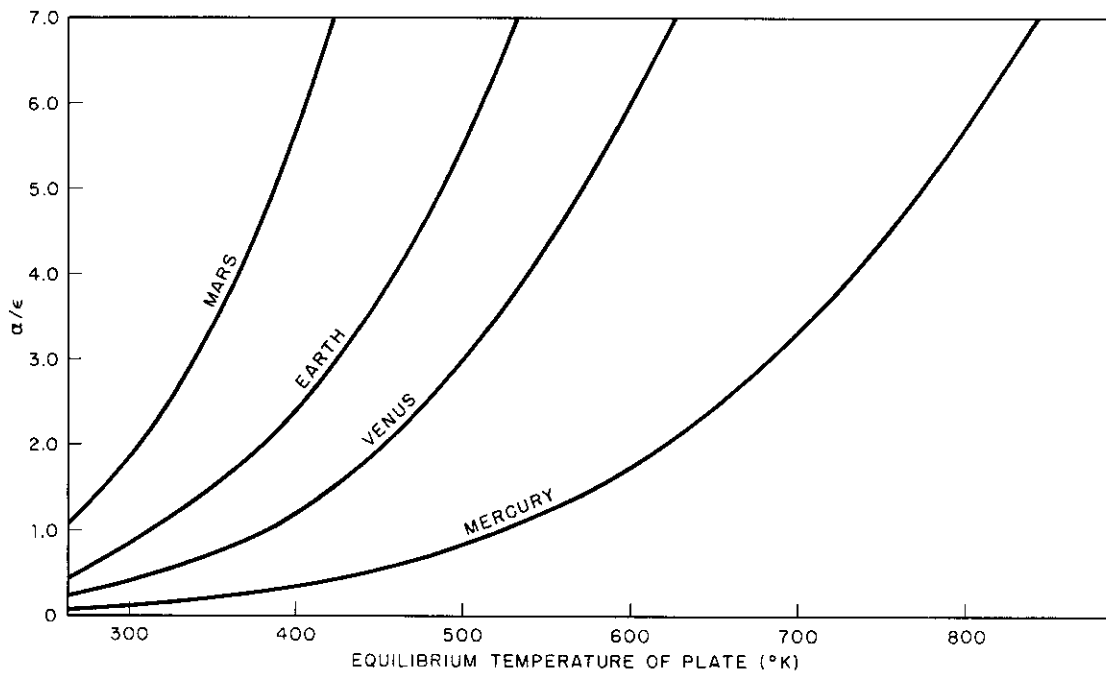


Fig. 1 Temperature equilibrium for a flat plate normal to the sun at various planetary distances.

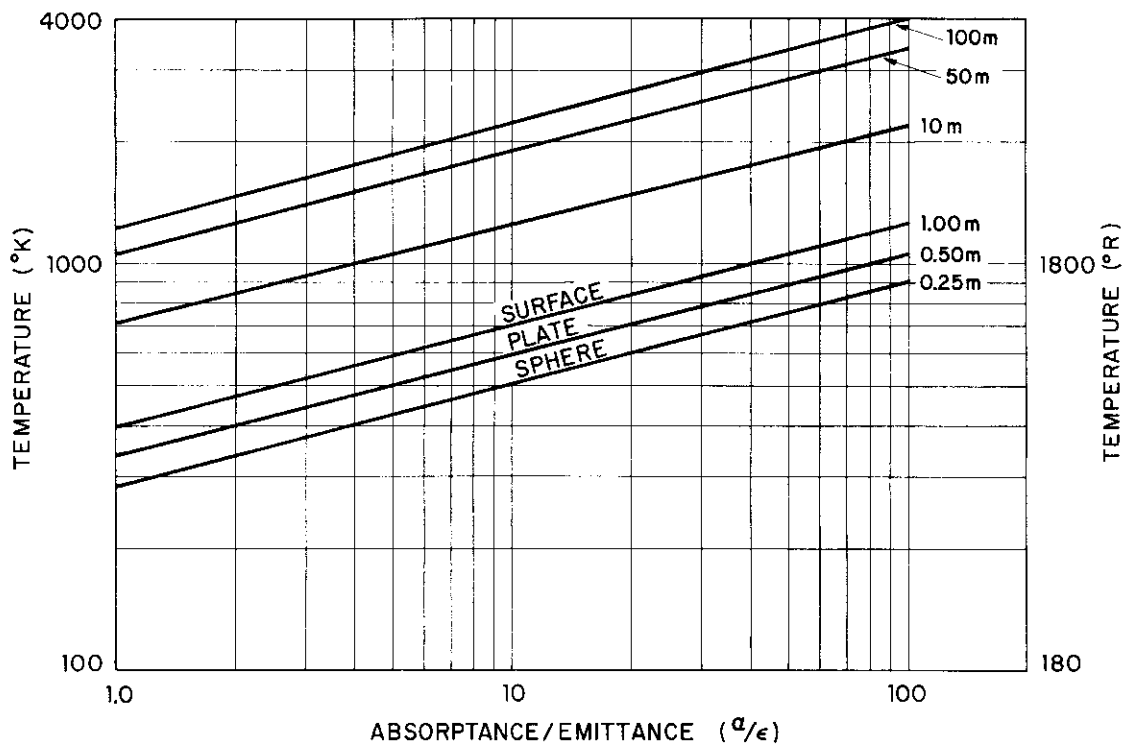


Fig. 2 Equilibrium temperatures in Earth's mean orbit.



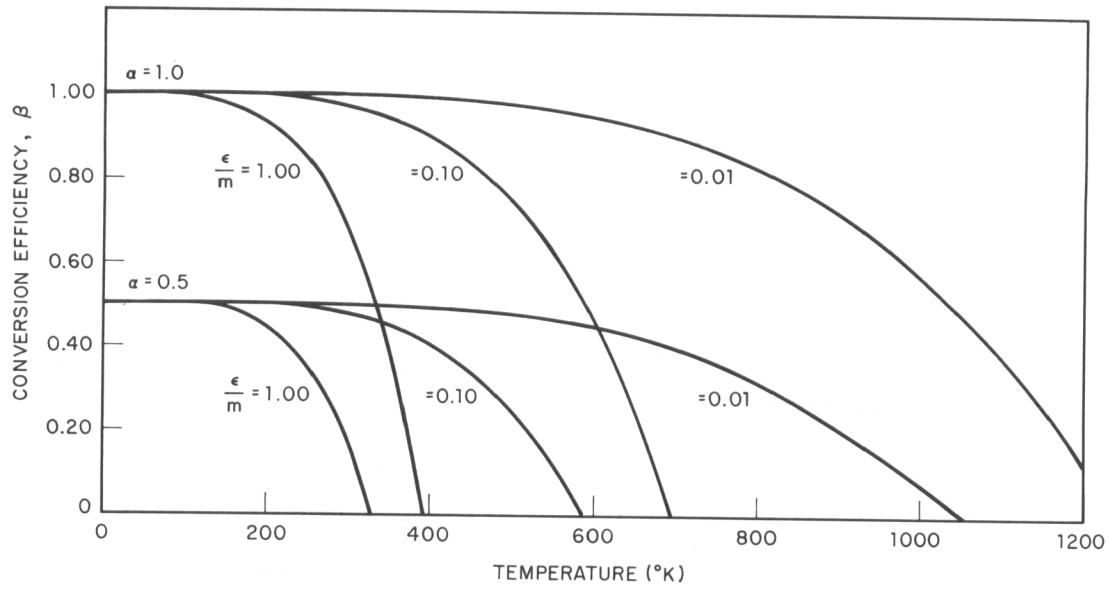


Fig. 3 Thermal conversion efficiencies for various temperatures in Earth's mean orbit.

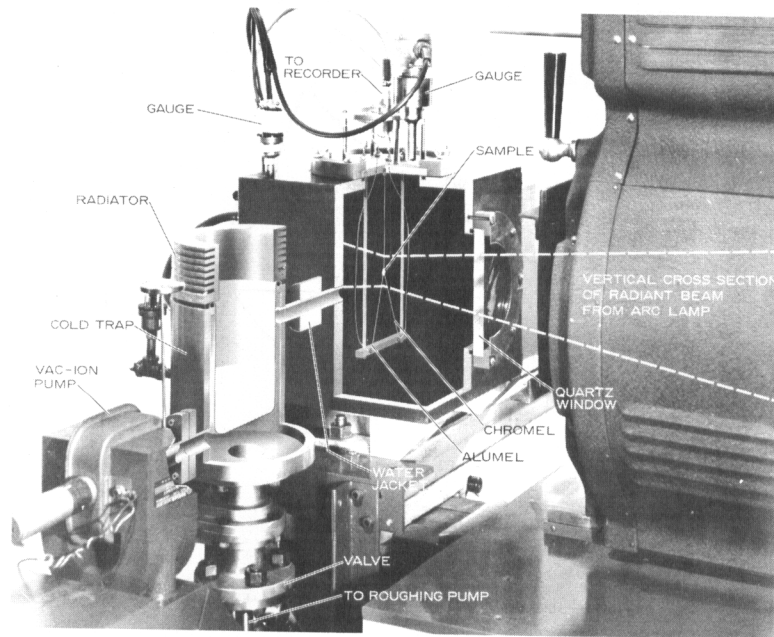


Fig. 4 Cut-away photograph of exposure chamber, showing specimen in beam.

# Contrails

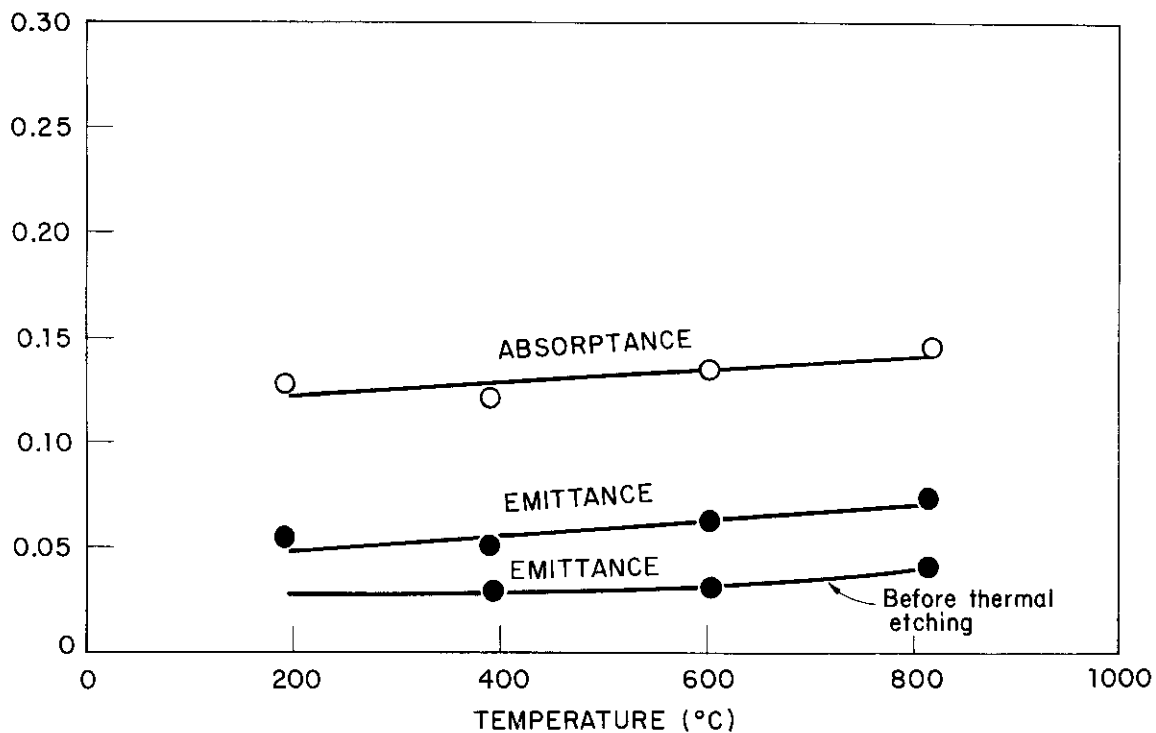


Fig. 5 Time-temperature record of specimen during exposure and cooling period.

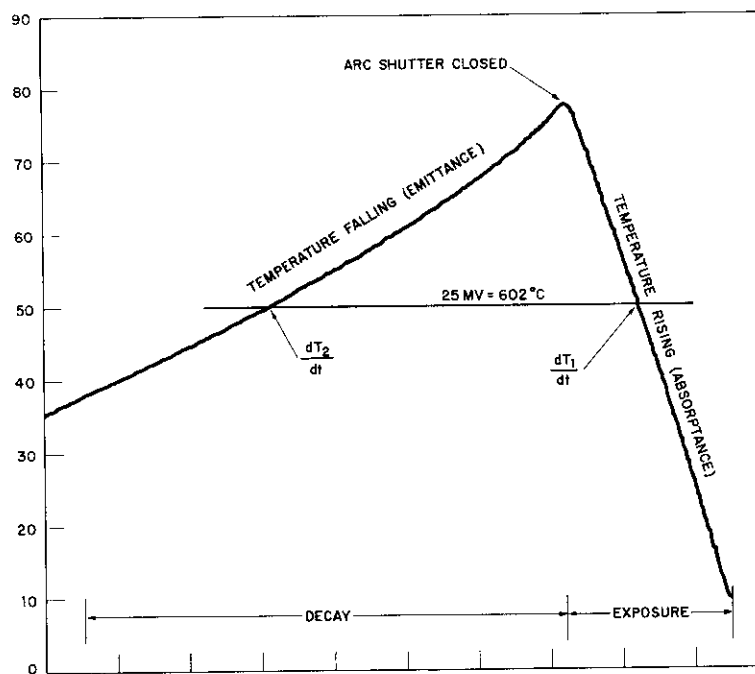


Fig. 6 Polished silver.

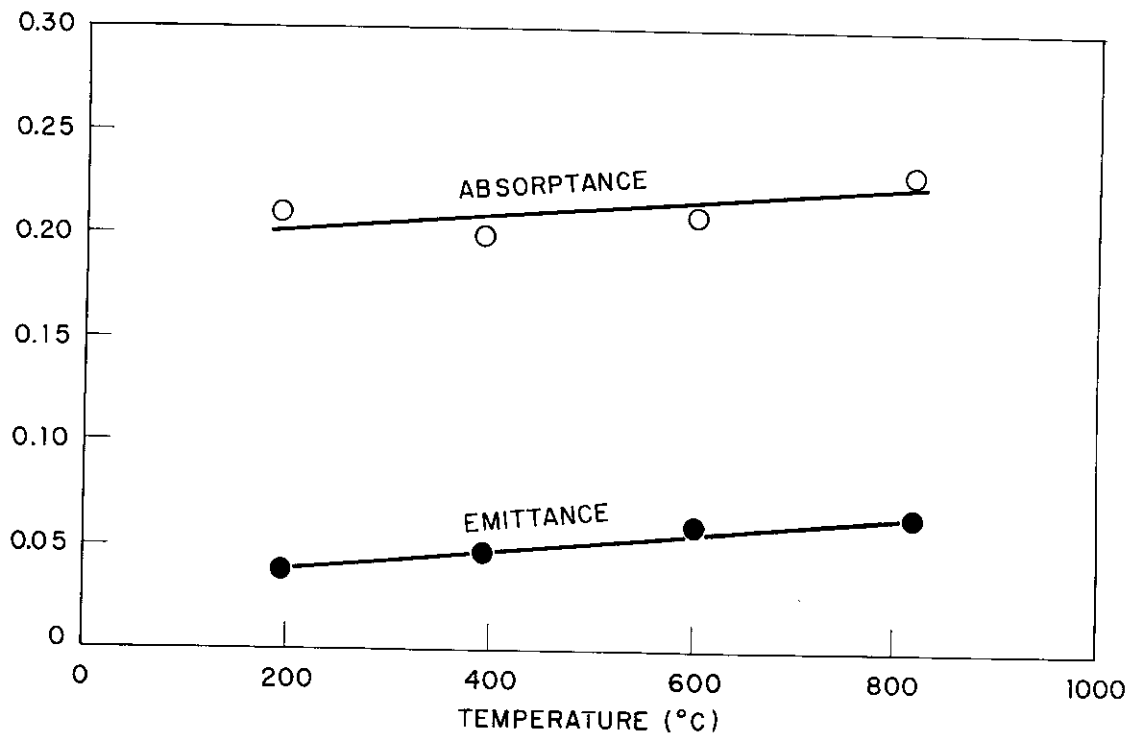


Fig. 7 Polished gold.

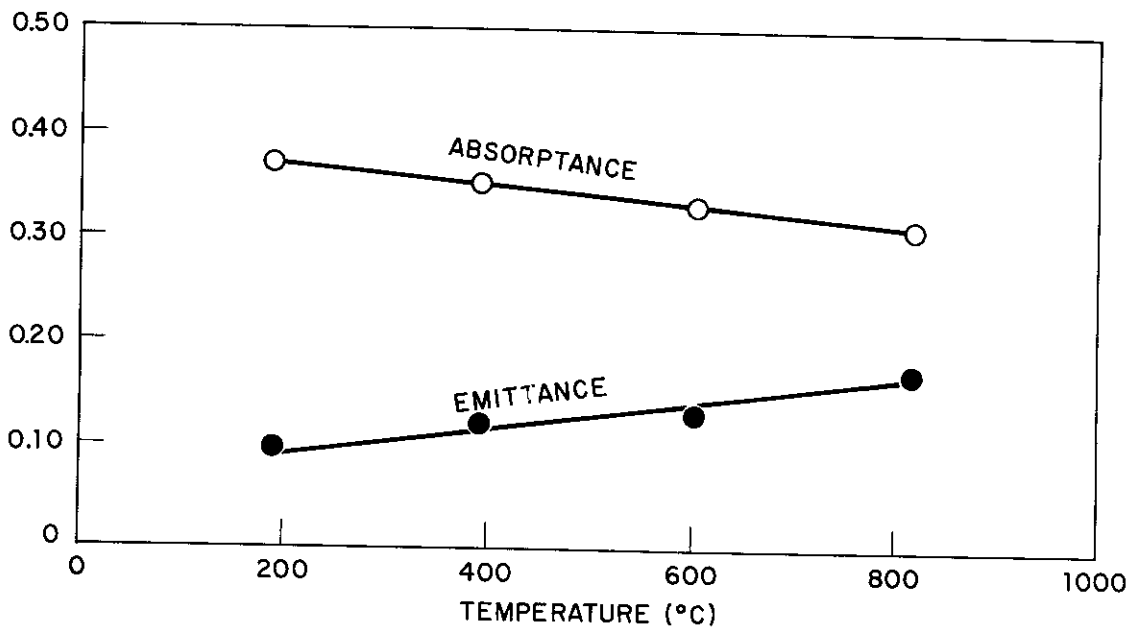


Fig. 8 Polished nickel.

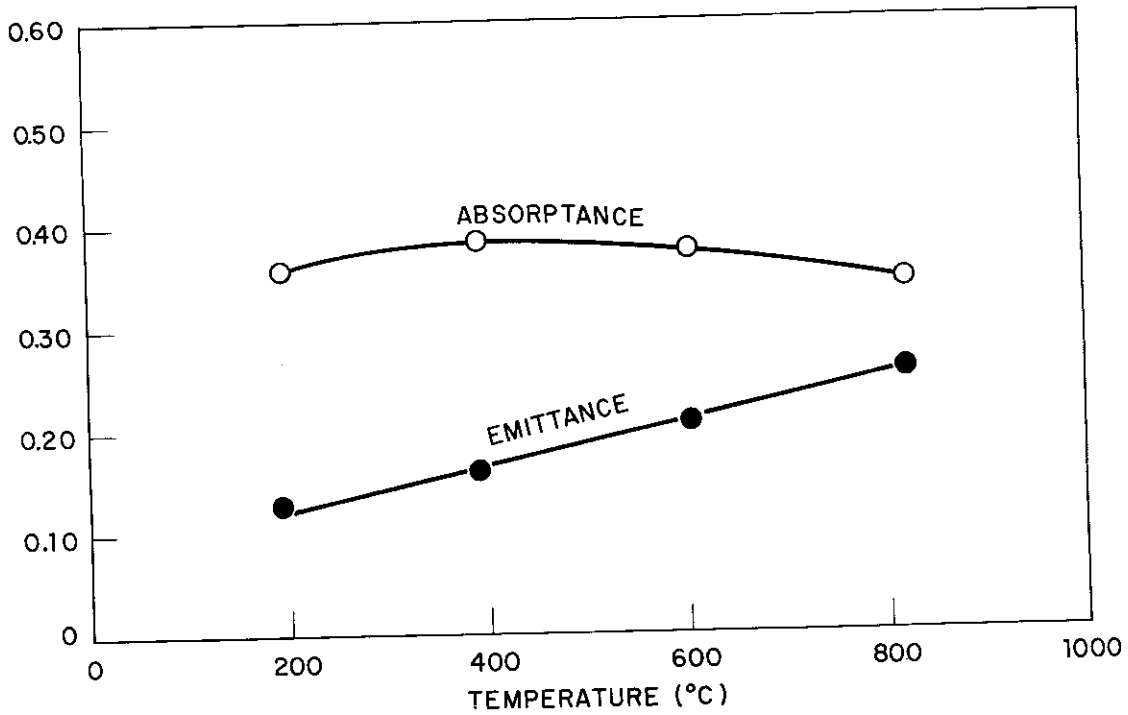


Fig. 9 Polished Armco iron.

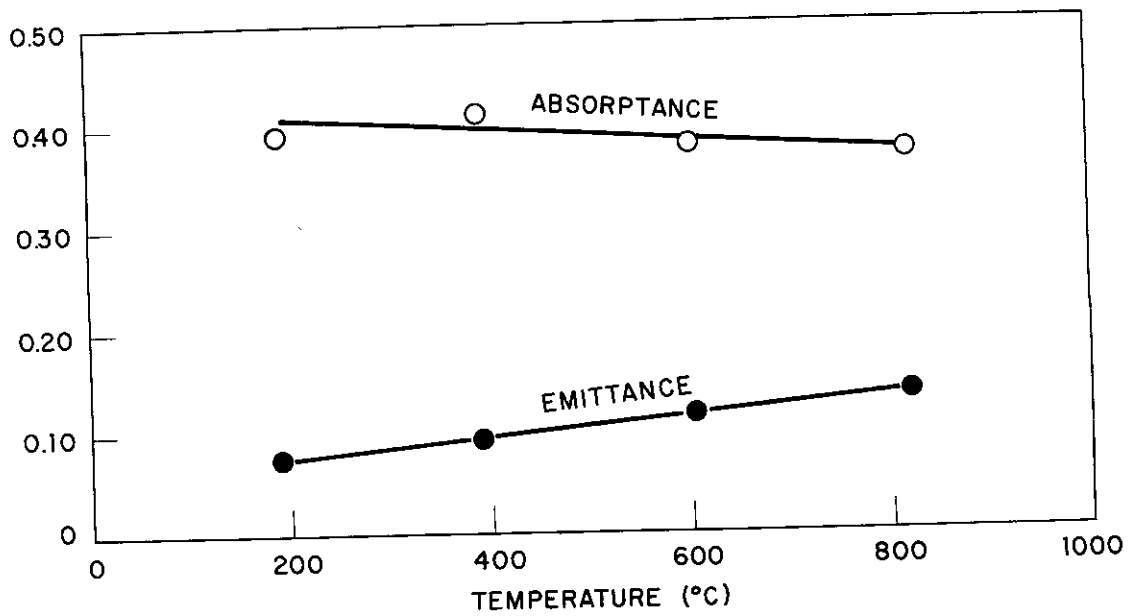


Fig. 10 Polished molybdenum.

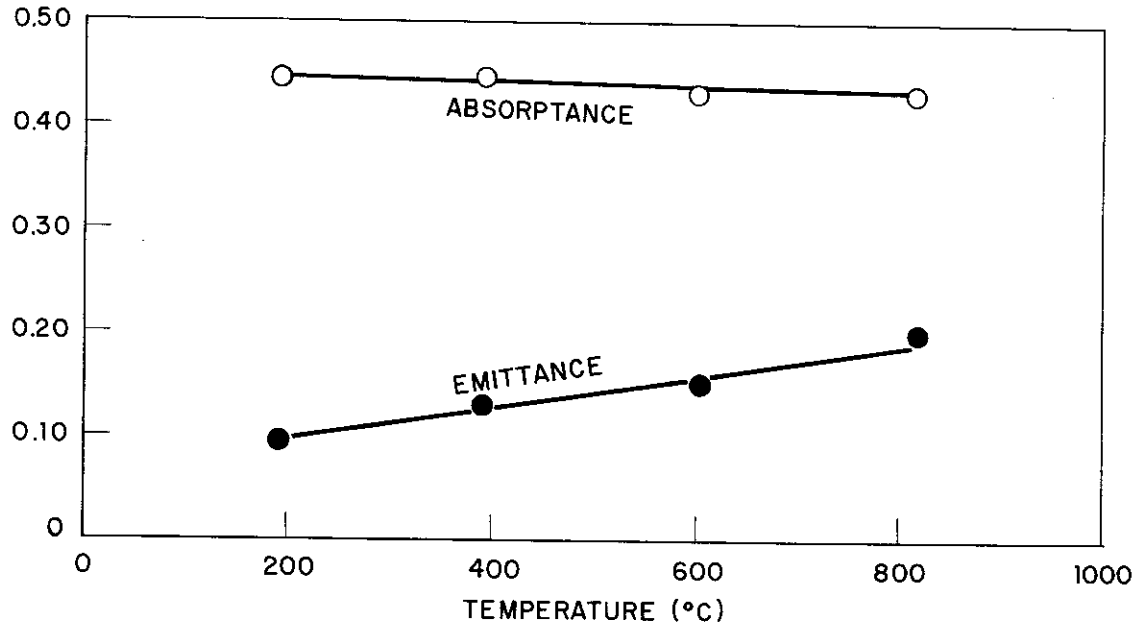


Fig. 11 Polished tantalum.

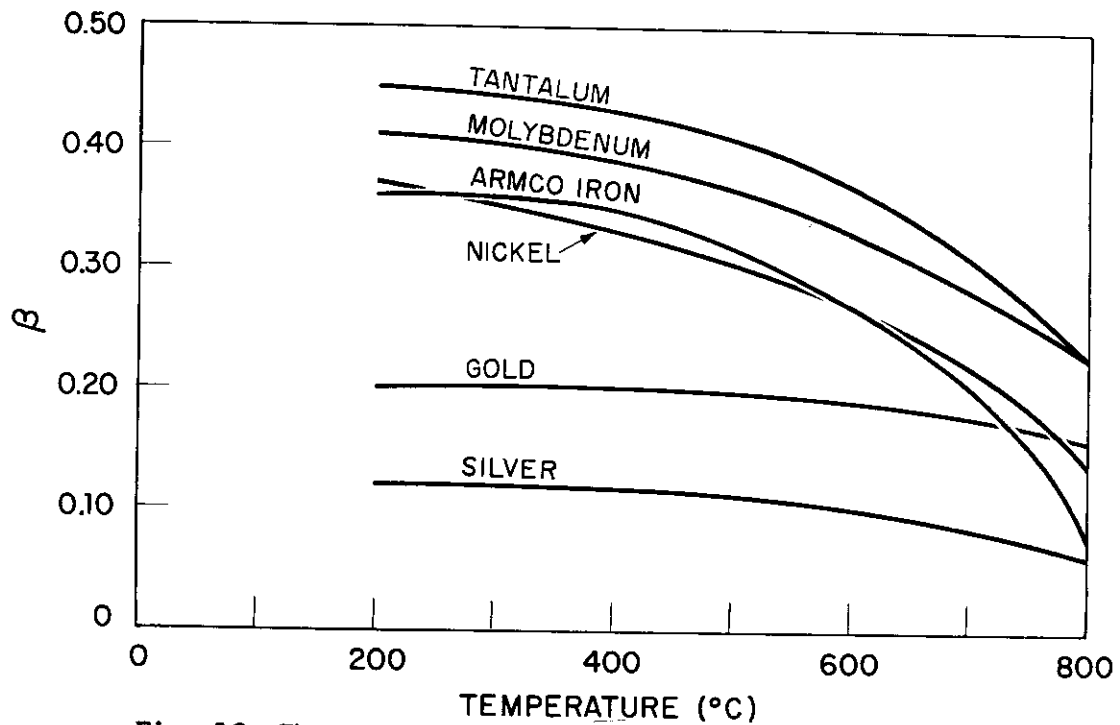


Fig. 12 Thermal efficiencies of polished metals.

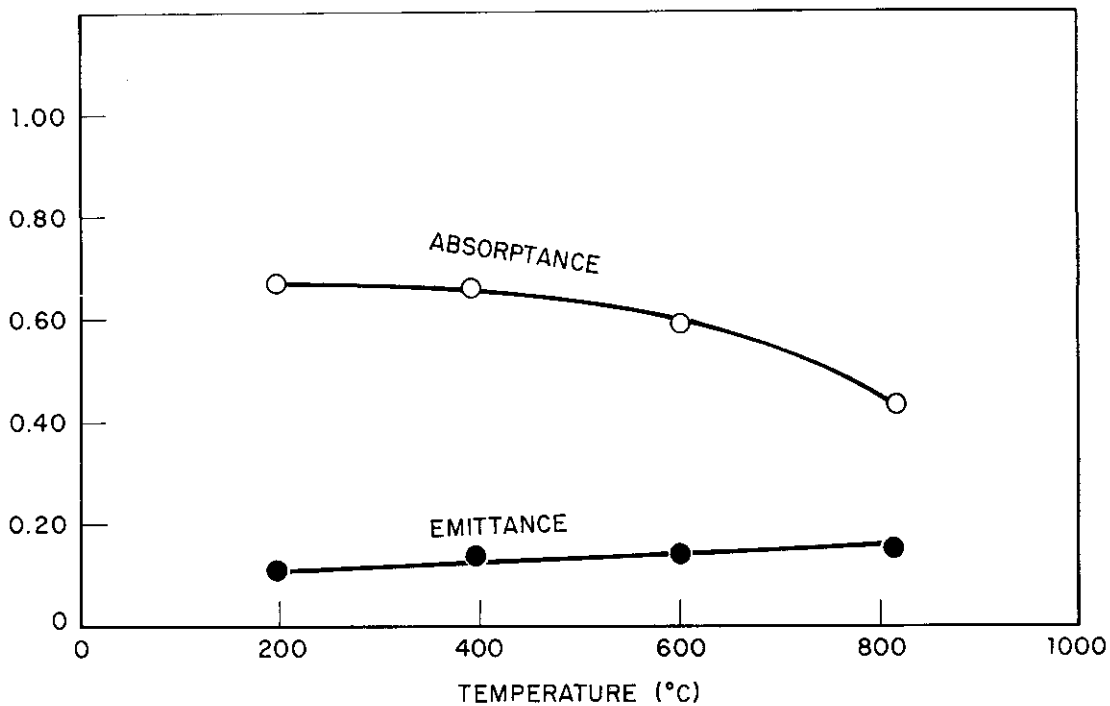


Fig. 13 Ag<sub>2</sub>S on silver.

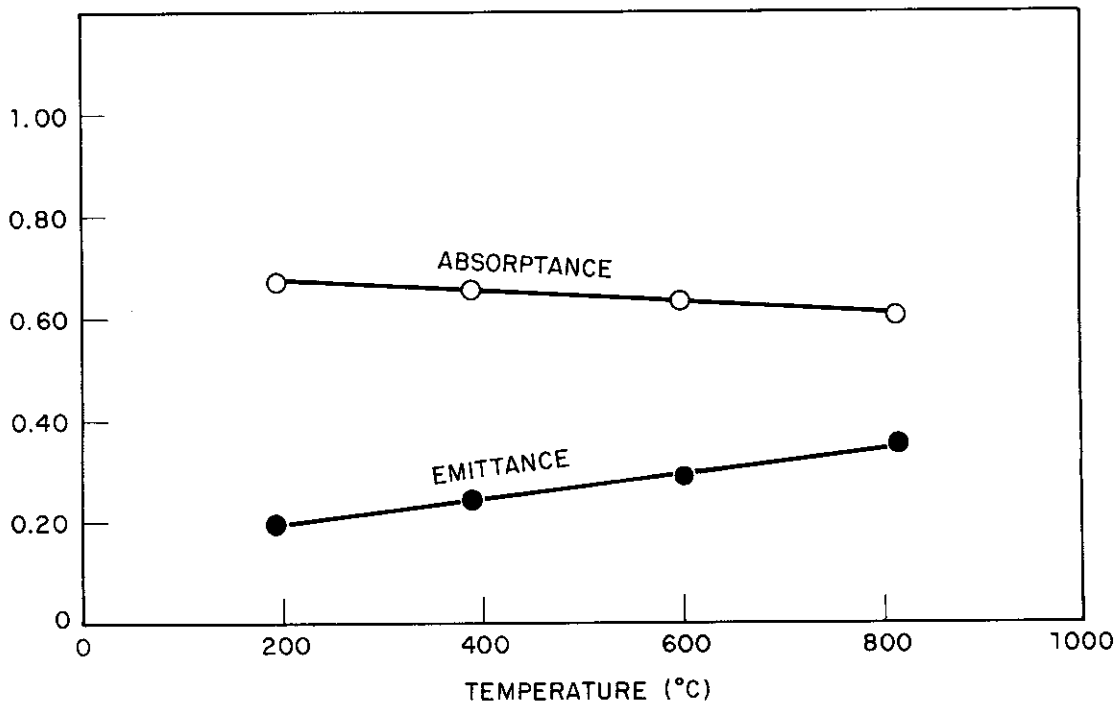


Fig. 14 Carbon coated molybdenum.



# Contrails

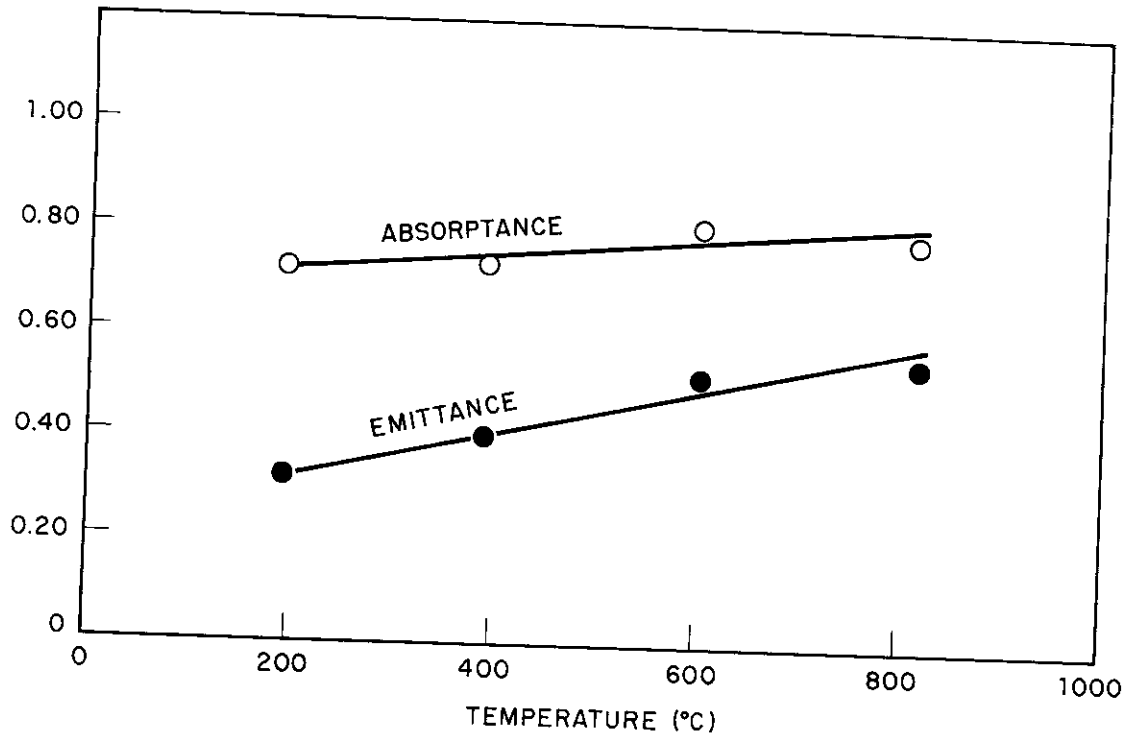


Fig. 15 Sandblasted Armco iron.

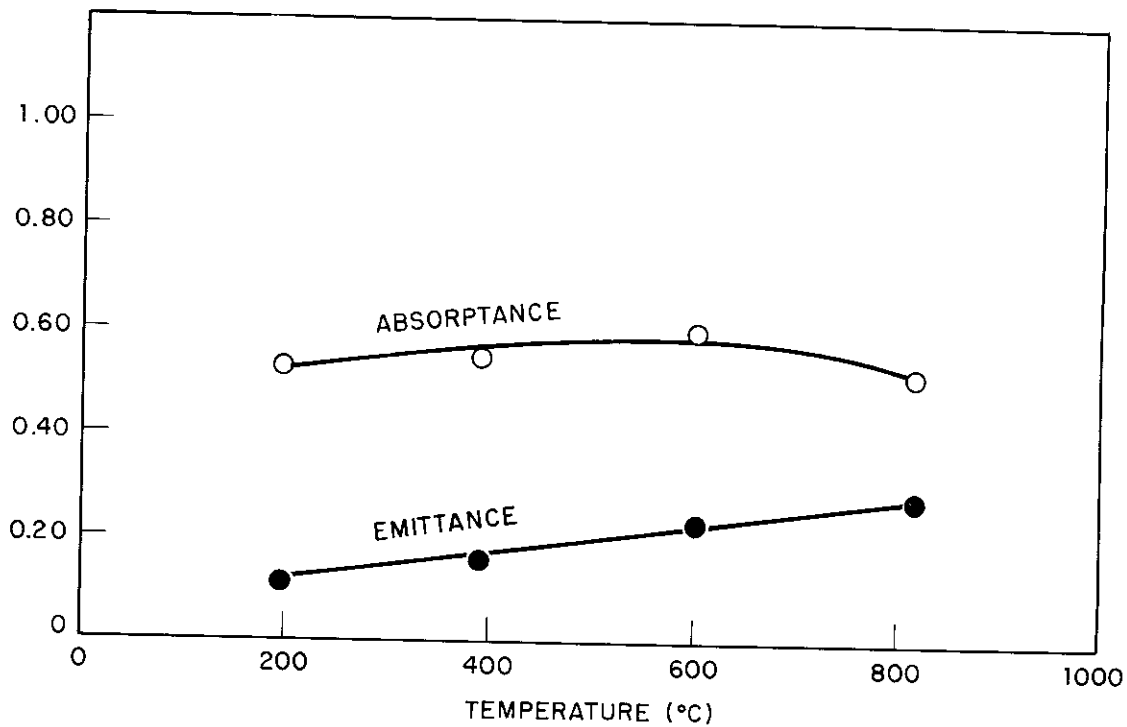


Fig. 16 Blued Armco iron.

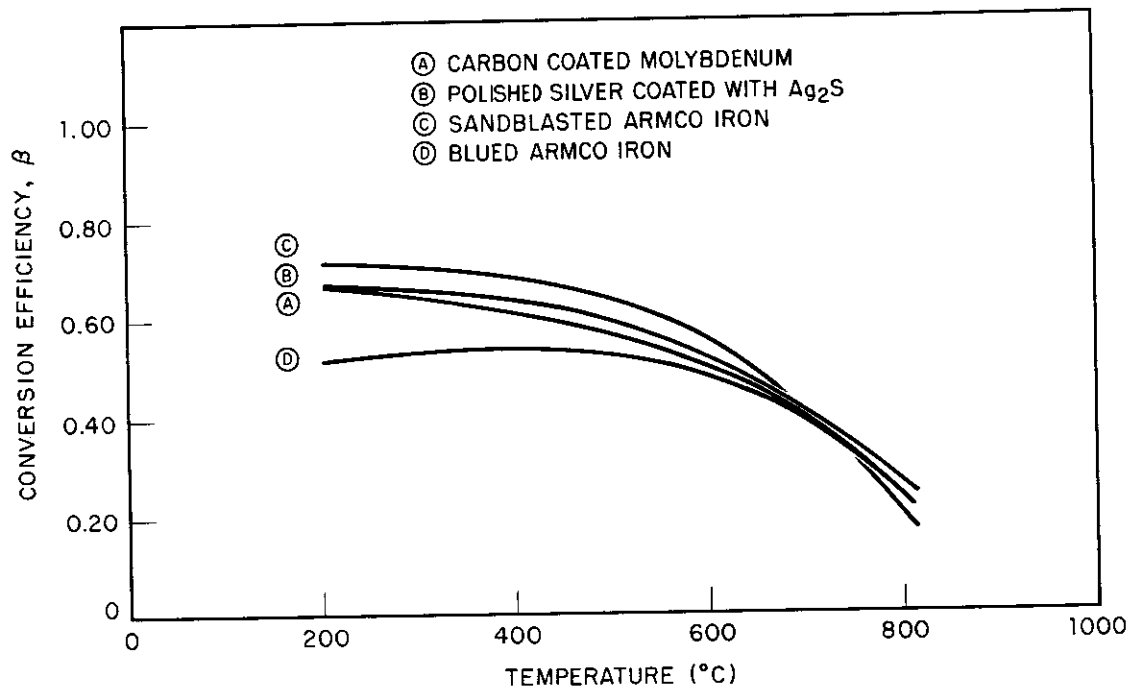


Fig. 17 Thermal efficiencies of coatings (Fig. 13, 14, 15, 16).

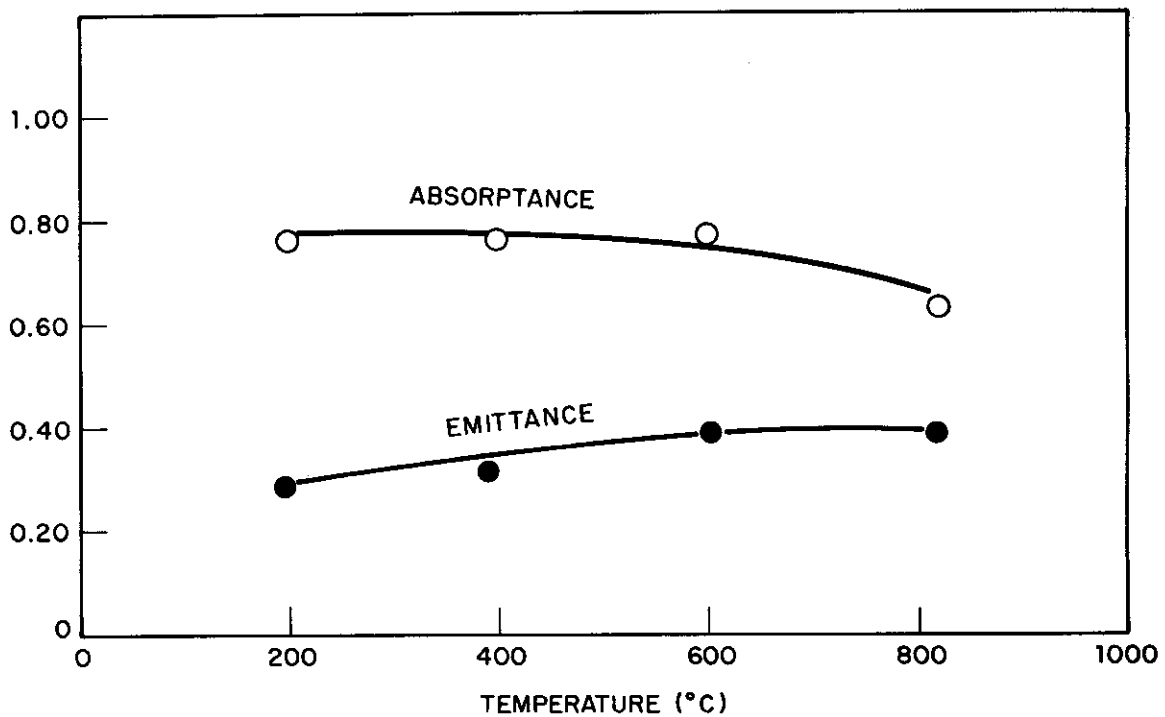


Fig. 18 Granular molybdenum on Armco iron.

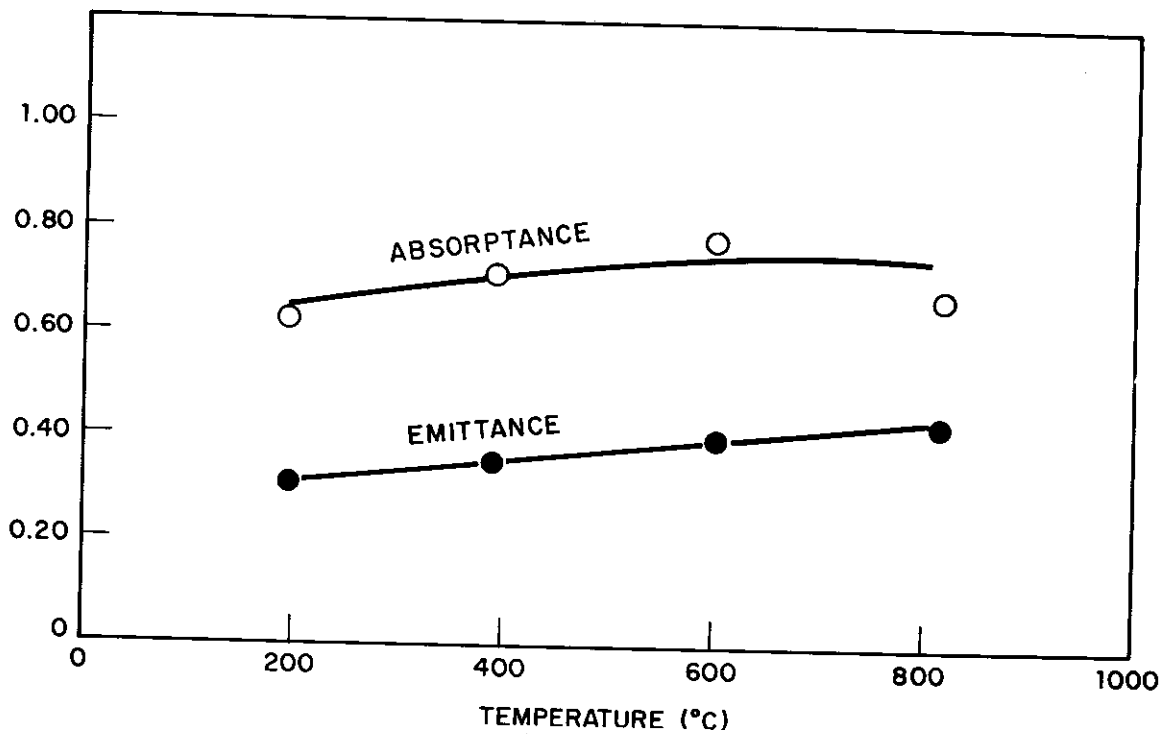


Fig. 19 Tungsten carbide on Armco iron.

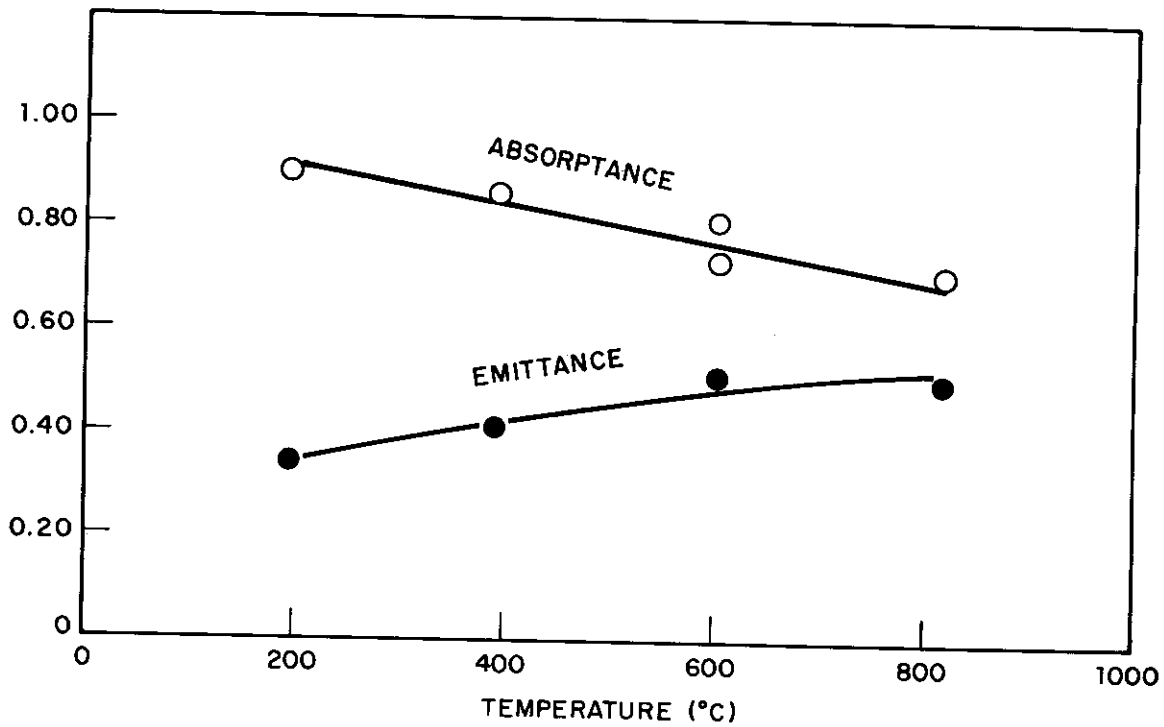


Fig. 20 Crystalline tungsten on Armco iron.

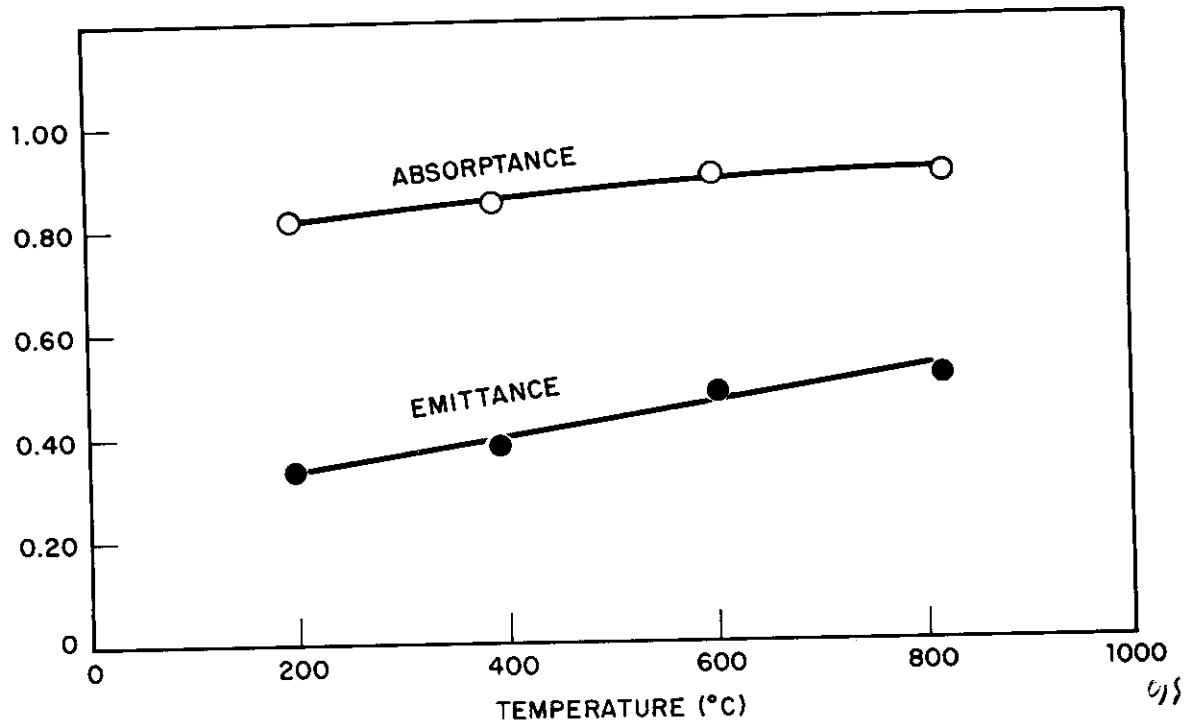


Figure 21 60% Chromium Carbide - Cobalt Blend on Armco Iron

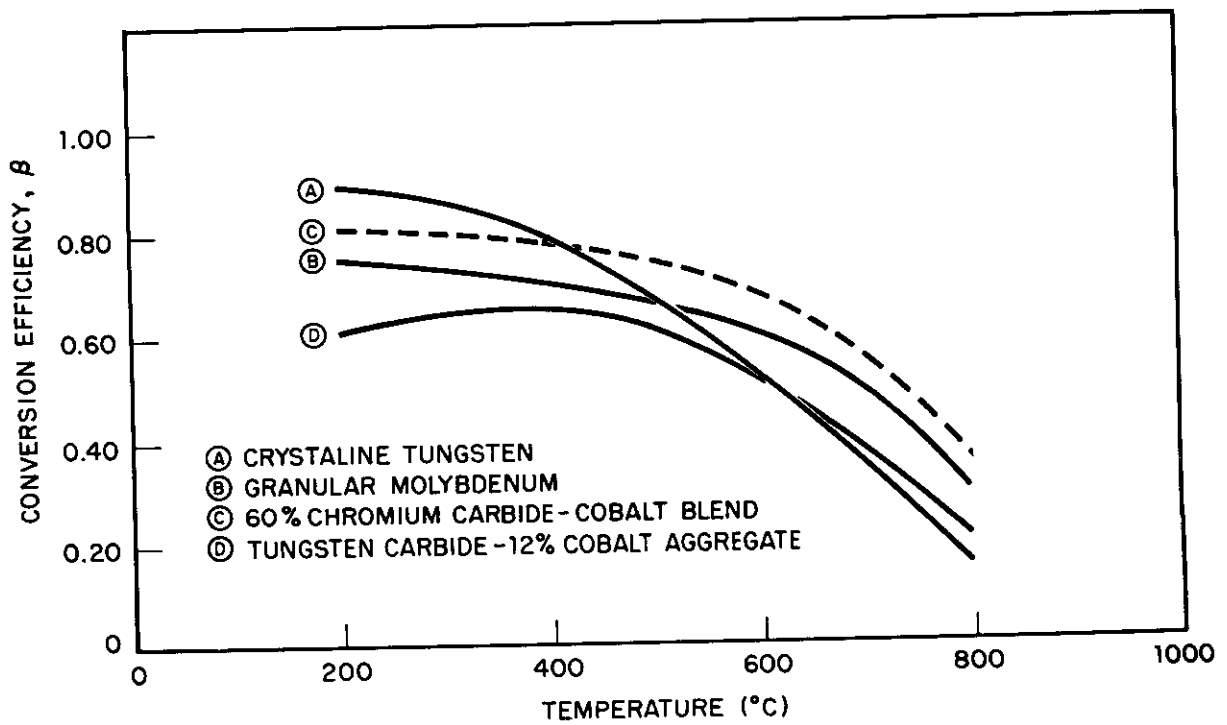


Figure 22 Thermal Efficiencies of Coatings